

OASIS: Online Sample Selection for Continual Visual Instruction Tuning

Minjae Lee^{1,*} Minhyuk Seo^{2,*} Tingyu Qu² Tinne Tuytelaars² Jonghyun Choi^{1,†}

¹ Seoul National University ² KU Leuven

{mj1020, jonghyunchoi}@snu.ac.kr

{minhyuk.seo, tingyu.qu, tinne.tuytelaars}@kuleuven.be

Abstract

In continual visual instruction tuning (CVIT) scenarios, where multi-modal data continuously arrive in an online streaming manner, training delays from large-scale data significantly hinder real-time adaptation. While existing data selection strategies reduce training overheads, they rely on pre-trained reference models, which are impractical in CVIT setups due to unknown future data. Recent reference model-free online sample selection methods address this issue but typically select a fixed number of samples per batch (*e.g.*, top- k), causing them to suffer from distribution shifts where informativeness varies across batches. To address these limitations, we propose OASIS, an adaptive online sample selection approach for CVIT that: (1) dynamically adjusts selected samples per batch based on relative inter-batch informativeness, and (2) minimizes redundancy of selected samples through iterative selection score updates. Empirical results across various MLLMs, such as LLaVA-1.5 and Qwen-VL-2.5, show that OASIS achieves comparable performance to full-data training using only 25% of the data and outperforms the state-of-the-art.

1 Introduction

Recent advances in LLMs (Yang et al., 2024; Liu et al., 2024a) have driven rapid progress in Multimodal Large Language Models (MLLMs) through vision-language alignments (Liu et al., 2023, 2024b; Guo et al., 2025). A key factor in their success is training on large-scale visual instruction tuning data (Bai et al., 2023b; Chen et al., 2023), with diverse multimodal tasks further improving generalization (Chen et al., 2024b). As high-quality visual instruction-tuning datasets continue to emerge (Maharana et al., 2025), MLLMs can now be trained on massive data to better adapt to user-specific preferences and contexts (Lau et al.,

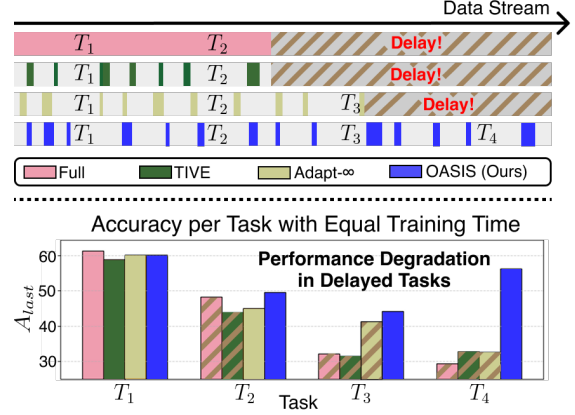


Figure 1: **Comparison of real-time adaptation under equal training time.** Width of the color bars in the data stream reflects training data volume. In the CVIT scenario, new tasks arrive continuously. ‘Full’ trains on all data, while TIVE (Liu et al., 2024c), Adapt- ∞ (Maharana et al., 2025), and our OASIS use 25% selected data. With equal training time, ‘Full’ suffers from training delays and fails to train on later tasks (*i.e.*, T_3 and T_4), leading to degraded performance. TIVE and Adapt- ∞ also struggle with later tasks due to selection overhead from backward passes. OASIS uses only forward passes, minimizing delay and achieving strong real-time adaptation.

2024; Zhang, 2024). However, larger-scale datasets increase the risks of overfitting and delays in training time (Ma et al., 2023; Liu et al., 2024c).

Unlike conventional learning setups, where MLLMs are fully trained on static datasets before deployment, real-world applications often involve continuous streams of new multi-modal data (Seo et al., 2024b). This necessitates ongoing adaptation to shifting data distributions, referred to as continual visual instruction tuning (CVIT) (Chen et al., 2024a; Maharana et al., 2025). Training delays in CVIT prevent the model from learning new data promptly, hindering real-time adaptation (Koh et al., 2022; Caccia et al., 2022). As shown in Fig. 1, full-data training delays the adaptation to newer tasks (T_3 and T_4) as the model spends exces-

*Equal contribution. † Corresponding author.

sive time training on earlier tasks (T_1 and T_2).

Data selection methods (Sorscher et al., 2022; Lee et al., 2024; Abbas et al., 2024) mitigate training delays by selecting informative subsets but typically rely on a reference model (Coleman et al., 2019; Mindermann et al., 2022; Shin et al., 2023) trained on the entire data in advance, which is infeasible in CVIT due to continuously arriving data and unknown future distributions. Reference model-free methods (Katharopoulos and Fleuret, 2018; Qin et al., 2024; Hong et al., 2024) address this issue by selecting the top- k scoring samples from each streaming batch without reference models.

While reference model-free methods eliminate reliance on reference models, they still face two main limitations: (i) failure to capture cross-batch informativeness: informative samples are unevenly distributed over time (Seo et al., 2025), with some batches containing many novel or forgotten samples, while others contain few, due to shifting data distributions; (ii) redundancy in selected subsets: similar instances often recur periodically (Koh et al., 2023) (e.g., Christmas data in winter, swimsuit data in summer), resulting in similar selection scores (Hong et al., 2024), which consequently leads to the selection of similar samples.

To address these limitations, we propose **Online Adaptive Sample selection via Informative Statistics (OASIS)**, which (i) adaptively adjusts the number of selected samples per batch based on informativeness, and (ii) reduces redundancy based on sample-wise similarity. Specifically, OASIS estimates each sample’s relative informativeness within the overall data distribution, whereas existing methods select top- k scoring samples per batches, ignoring inter-batch differences. Moreover, since high-scoring samples within a batch often exhibit redundancy (Hong et al., 2024), OASIS iteratively updates selection scores. Each time a sample is selected, it adjusts for shared information among previously selected samples. OASIS efficiently select samples by requiring only a forward pass, which incurs roughly half the cost of backward passes (Huo et al., 2018). As shown in Fig. 1, OASIS outperforms prior methods by overcoming training delays while maintaining strong performance throughout training.

We empirically validate OASIS by comparing it with recent sample selection baselines across various MLLMs, such as LLaVA-1.5-7B (Liu et al., 2024b) and Qwen-VL-2.5-7B (Bai et al., 2025), on multiple CVIT benchmarks. In particular, OASIS

incurs only a 1.51% performance degradation compared to full-data training (i.e., without sample selection), while training with only 25% of samples on MICVIT benchmark.

We summarize our contributions as follows:

- We propose an adaptive sample selection strategy that selects batch samples based on their informativeness relative to the entire dataset, moving beyond batch-wise selection.
- We propose a redundancy reduction strategy that leverages sample-wise similarity to minimize redundancy among selected samples.
- By combining two strategies, our proposed OASIS significantly outperforms baselines in CVIT through extensive evaluations.

2 Related Work

Continual Visual Instruction Tuning in MLLMs.

Existing visual instruction tuning methods often focus on fixed tasks (Zhu et al., 2024; Bai et al., 2025), overlooking continuously emerging visual instruction data (Maharana et al., 2025; Guo et al., 2025). To adapt MLLMs to dynamically changing data distributions, *continual visual instruction tuning* (CVIT) has been proposed, which aims to learn new tasks while preserving knowledge from previously encountered instruction data (He et al., 2023). To reflect real-world distribution shifts, various CVIT benchmarks (e.g. COAST (Cao et al., 2024), UCIT (Guo et al., 2025)) and strategies (e.g. Fwd-Prompt (Zheng et al., 2024), SEFE (Chen et al., 2025)) have been proposed. However, they train MLLMs on all data, leading to overfitting (Rice et al., 2020; Zhai et al., 2023), high computational costs (Wang et al., 2024; Panos et al., 2025), and training delays (Caccia et al., 2022; Ghunaim et al., 2023). Although aL-SAR (Seo et al., 2025) improves efficiency through dynamic layer freezing based on batch informativeness, it still uses the full dataset, limiting its overall efficiency.

Data Selection. Motivated by the observation that not all data contribute equally to learning, recent work explores selecting informative subsets to match full-data performance with lower training cost (Lee et al., 2024; Abbas et al., 2024; Qin et al., 2024). Bayesian (Deng et al., 2023b) and RHO-LOSS (Mindermann et al., 2022) improve efficiency by data selection but require a reference model pretrained on the full dataset. TIVE (Liu et al., 2024c) uses smaller reference data, but requires full-layer gradient computation, incurring

high computational overhead. This reliance on reference models limits their use in CVIT, where sequentially arriving data makes full-data pretraining infeasible. To address this, reference model-free online sample selection methods like GradNorm (Katharopoulos and Fleuret, 2018), InfoBatch (Qin et al., 2024), and DivBS (Hong et al., 2024) have been proposed. However, they select a fixed number of samples per batch based on difficulty or dissimilarity, limiting adaptability to varying data distributions, where some batches may contain more informative samples (*e.g.*, newly encountered or forgotten) than others. SelfSup (Sorscher et al., 2022), COINCIDE (Lee et al., 2024), and DBP (Abbas et al., 2024) select samples by K -means clustering with a sensitive hyperparameter K , which is difficult to tune under non-i.i.d. streams due to representation shifts (Książek et al., 2025). Adapt- ∞ (Maharana et al., 2025) assumes known task boundaries and relies on costly intermediate gradients, limiting its real-world applicability.

3 Approach

We first present the problem statement for online sample selection in CVIT in Sec. 3.1. We then introduce our method, **Online Adaptive Sample selection via Informative Statistics (OASIS)**, in Sec. 3.2, which consists of two components: **Online Relative Informativeness Selection (ORIS)** in Sec. 3.3 and **Similarity-aware Information Redundancy Elimination (SIREN)** in Sec. 3.4.

3.1 Online Sample Selection in CVIT

Continual Visual Instruction Tuning (CVIT) trains an MLLM on a data stream \mathcal{D} comprising a sequence of T tasks, *i.e.*, $\mathcal{D} = \mathcal{D}_1, \dots, \mathcal{D}_T$, where each $\mathcal{D}_i = \{(x_1^i, y_1^i), (x_2^i, y_2^i), \dots\}$ represents the training dataset for task i . Reflecting real-world scenarios where data are collected continuously over time (Koh et al., 2022), online CVIT assumes that data arrive as an online stream of samples, denoted as $(x_1^i, y_1^i), (x_2^i, y_2^i), \dots$, while the chunk of task \mathcal{D}_i is provided at once in offline CVIT. At timestep t , a batch B_t with batch size N_B is drawn from \mathcal{D} . Then, a subset $\mathcal{B}_t^* \subset B_t$, consisting of N_s samples ($N_s < N_B$), is selected according to a predefined selection ratio, and only this selected subset is used for training. Given the parameters θ of an MLLM f and a loss function \mathcal{L} , the training

objective is formulated as:

$$\min_{\theta} \mathbb{E}_{B_t \sim \mathcal{D}} [\mathcal{L}(f_{\theta}(\mathcal{B}_{t,x}^*), \mathcal{B}_{t,y}^*)]. \quad (1)$$

3.2 Online Adaptive Sample Selection via Informative Statistics

Existing online sample selection methods typically select a fixed number of samples per batch, *e.g.*, top- N_s selection scores, which struggles under distribution shifts (*e.g.*, CVIT), due to: (i) the number of informative samples per batch varying over time, and (ii) similar samples (*e.g.*, samples from the same task) tend to be encountered together within a batch and may have similar scores (Hong et al., 2024), causing redundancy among selected samples. To address these limitations, we propose two strategies: (i) **Online Relative Informativeness Selection (ORIS)**, which adaptively selects samples based on their relative informativeness across the entire data distribution, rather than considering only intra-batch comparisons; and (ii) **Similarity-aware Information Redundancy Elimination (SIREN)**, which reduces redundancy by adjusting sample informativeness based on sample-wise gradient similarity.

Specifically, for each training batch, ORIS computes sample-wise informativeness using Fisher Information (FI) and estimates relative informativeness within the overall FI distribution. During this calculation, SIREN adjusts these scores using sample-wise gradient similarity to account for the impact of training one sample on others. Integrating ORIS and SIREN, we call our method **Online Adaptive Sample selection via Informative Statistics (OASIS)**. We provide an overview of OASIS in Fig. 2, and pseudocode in Sec. A.13.

3.3 Online Relative Informativeness Selection

Informativeness I . To select informative samples, we first define the sample-wise informativeness I based on Fisher Information (FI), which quantifies potential model information gain from data (Deng et al., 2023a; Kirsch and Gal, 2022). However, calculating full FI requires both forward and backward processes, negating the efficiency advantage of training only on a selected subset of samples. Therefore, we approximate it by: (i) computing it solely at the last layer L , as gradients of preceding layers are proportional to it by the chain rule (Koh et al., 2023); and (ii) using a first-order approximation with diagonal components of the FI matrix, avoiding Hessian computation (Kirkpatrick

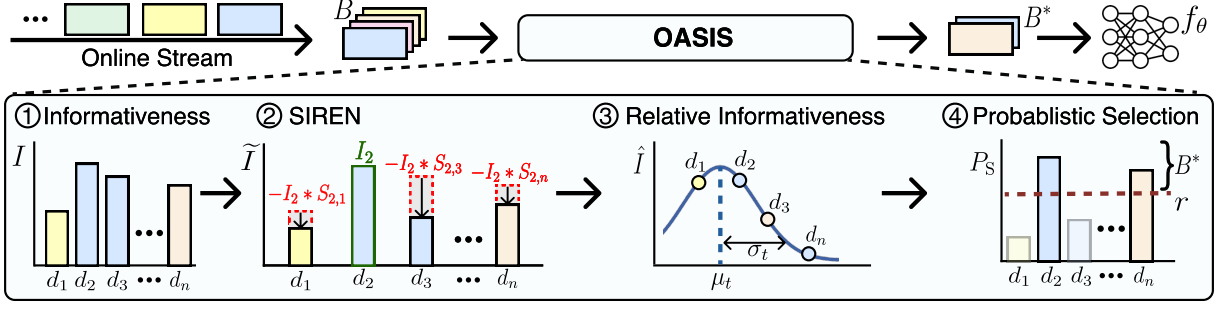


Figure 2: **Overview of our proposed OASIS.** For each online batch B : (1) OASIS first scores the informativeness I for all sample in batch B (Sec. 3.3); (2) It then iteratively reduces redundancy by adjusting I of other samples to \tilde{I} based on their gradient similarity $S_{i,j}$ to the most informative sample d_i . (Sec. 3.4); (3) OASIS computes relative informativeness \hat{I} by normalizing the updated informativeness \tilde{I} using EMA μ_t and EMV σ_t (Sec. 3.3); (4) Finally, OASIS computes selection probability P_S and selects samples exceeding a uniformly drawn threshold r , resulting in a selected subset $B^* \subset B$ (Sec. 3.3). Model f_θ is then trained using only the selected subset B^* .

et al., 2017; Soen and Sun, 2021). Formally, we define the informativeness $I_i^{(t)}$ of the i th sample $d_i^{(t)} = (x_i^{(t)}, y_i^{(t)})$ in batch B_t as:

$$I_i^{(t)} = \text{tr} \left[\left(\nabla_{\theta_L} L(d_i^{(t)}) \right) \cdot \left(\nabla_{\theta_L} L(d_i^{(t)}) \right)^\top \right], \quad (2)$$

where $L(d_i^{(t)}) = \ell(f_\theta(x_i^{(t)}), y_i^{(t)})$, ℓ is the loss function, θ_L is the last-layer parameters of the MLLM $f_\theta(\cdot)$, and $\text{tr}(\cdot)$ denotes the trace operator. While existing methods use gradients from middle (Maharana et al., 2025) or all layers (Liu et al., 2024c), incurring costs comparable to full-data training, ORIS substantially reduces overhead through approximate forward passes, minimizing expensive gradient computations.

Relative Informativeness \hat{I} . However, we cannot compare I across different batches, as θ in Eq. 2 changes over time due to model updates at each batch iteration. In other words, cross-batch comparison of I would require re-forwarding all previously encountered samples, incurring substantial computational overhead and being infeasible in online CVIT scenarios where previous samples may be discarded (Maharana et al., 2025). To avoid these issues, instead of tracking all samples' I , we estimate each sample's relative position with respect to the average I of encountered samples.

Specifically, since I from earlier time steps becomes outdated compared to recent ones, we maintain exponential moving average (EMA) and variance (EMV) of I , inspired by the exponential decay model of forgetting (Shin and Lee, 2020; Mahto et al., 2020; Chien et al., 2021). Formally, at each timestep t , given batch B_t of size N_B and decay

factor α , we update EMA μ_t and EMV σ_t of I as:

$$\mu_t = \alpha \bar{I}^{(t)} + (1 - \alpha) \mu_{t-1}, \quad (3)$$

$$\sigma_t = \alpha (\bar{I}^{(t)} - \mu_{t-1})^2 + (1 - \alpha) \sigma_{t-1}, \quad (4)$$

where $\bar{I}^{(t)} = \frac{1}{N_B} \sum_{i=1}^{N_B} I_i^{(t)}$ denotes average $I^{(t)}$ of samples in B_t .

Using exponential statistics, we estimate each sample's relative informativeness over all previously observed data. As empirical evidence shows that I of observed data approximates a normal distribution (Fig. 3), we apply Z-score normalization to I to quantify a sample's deviation from the overall I distribution. Formally, we define Relative Informativeness $\hat{I}^{(t)}$ of the i th sample with informativeness $I_i^{(t)}$ in batch B_t at time step t as:

$$\hat{I}_i^{(t)} = \frac{I_i^{(t)} - \mu_t}{\sigma_t}. \quad (5)$$

Probabilistic Selection. We then determine whether to select each sample based on $\hat{I}^{(t)}$. Inspired by coreset approaches (Bang et al., 2021; Seo et al., 2024a), which select not only informative but also easy-to-learn samples, we adopt probabilistic selection based on \hat{I} rather than deterministically selecting samples where $\hat{I} > I_T$, with the threshold Z-score I_T determined by the target selection ratio. Specifically, we apply Sigmoid to $\hat{I} - I_T$, and perform Bernoulli sampling, allowing inclusion of samples below the threshold. Formally, with uniform random threshold $r \sim \mathcal{U}(0, 1)$ where $\mathcal{U}(0, 1)$ denotes the standard uniform distribution over the interval $[0, 1]$, we define the selected samples set B_t^* from batch B_t as:

$$B_t^* = \{d_i^{(t)} \in B_t \mid \text{sigmoid}(\hat{I}_i^{(t)} - I_T) > r\}. \quad (6)$$

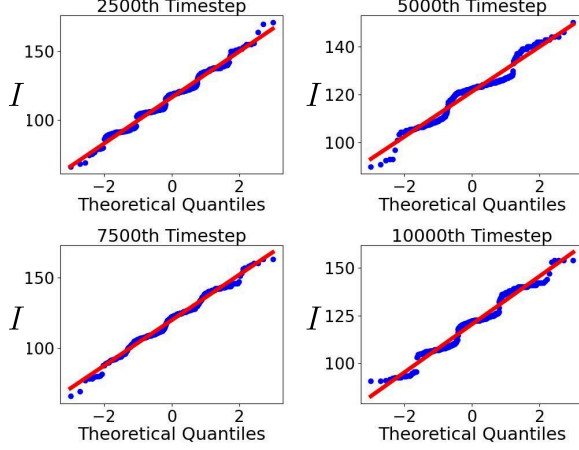


Figure 3: **QQ Plot of informativeness I .** We measure I on 500 randomly selected samples from those encountered at each training timestep. Each blue dot represents a sample, and the red line indicates the expected normal distribution. The close alignment of dots with the line suggests that I is approximately normally distributed.

Note that existing online batch selection methods require prior knowledge of the total sample count to set per-batch selection quotas for the desired selection portion. In contrast, our proposed ORIS selects samples where $\hat{I}_i > I_T$, with I_T set solely by the selection ratio, enabling use in endless real-world data streams. We provide details on determining I_T in Sec. A.6.

3.4 Similarity-Aware Information Redundancy Elimination

In real-world data streams, similar task data tend to arrive together. Therefore, selecting samples within B_t using ORIS without considering intra-batch similarity may result in redundant selections. To reduce redundancy, we adjust I based on sample-wise similarity. Ideally, we would iteratively train with the most informative sample in a batch, then recompute I for the remaining batch samples, as training on similar samples reduces the informativeness of related ones (Hekimoglu et al., 2023), thereby reducing redundancy. However, this introduces excessive computational overhead by requiring re-computation of I for every selection and makes batch-wise training impractical.

Instead, we approximate the change in I without re-forwarding. Inspired by Du et al. (2018); Seo et al. (2025), which demonstrate that gradient alignment correlates with informational overlap, we use gradient similarity to assess redundancy among samples in a batch. Specifically, we iteratively update each sample’s I to simulate the change, as-

suming the model has already been trained on previously identified high-informative samples. Given a batch $B_t = \{d_1^{(t)}, d_2^{(t)}, \dots, d_B^{(t)}\}$, we first calculate I for each sample and sort them in descending order, i.e., $I_0^{(t)} > I_1^{(t)} > \dots > I_B^{(t)}$. Then, we add the most informative sample (i.e., d_0) to the set H , where H is the set we assume has been used for training. For each remaining sample $d_i^{(t)} \in B_t \setminus H$, we define updated informativeness $\tilde{I}_i^{(t)}$ as:

$$\tilde{I}_i^{(t)} = I_i^{(t)} - \sum_{h \in H} \cos(g_i, g_h) \cdot I_h, \quad (7)$$

where $g_i = \nabla \ell_{\theta_L}(f(x_i), y_i)$ refers to the last-layer gradient of sample $d_i = (x_i, y_i)$. We iteratively add d_0, d_1, \dots, d_B to H and repeat the process iteratively, as shown in Algorithm 1.

However, when $|H| > 1$, overlapping similarities between samples in H cause duplicate subtractions. We resolve this using the inclusion-exclusion principle to capture higher-order redundancy as:

$$\begin{aligned} \tilde{I}_i^{(t)} = I_i^{(t)} &- \sum_{h \in H} \cos(g_i, g_h) \cdot I_h \\ &+ \sum_{\substack{U \subseteq H \\ |U| \geq 2}} (-1)^{|U|} \cos(g_i, \bar{g}_U) \cdot \bar{I}_U, \end{aligned} \quad (8)$$

where U denotes all possible non-empty subset of H with $|U| > 1$, $\bar{g}_U = \frac{1}{|U|} \sum_{u \in U} g_u$ and $\bar{I}_U = \frac{1}{|U|} \sum_{u \in U} I_u$ denote the average gradient and average I over subset $U \subseteq H$, respectively.

We use $\tilde{I}^{(t)}$ to calculate relative informativeness $\hat{I}^{(t)}$ instead of directly using $I^{(t)}$, as shown in Fig. 2. By applying SIREN before computing $\hat{I}^{(t)}$ in ORIS, we effectively reduce redundancy without requiring any re-forwarding process.

4 Experiments

4.1 Experimental Setup

In all experiments, we report the mean and standard deviation of the results from three different seeds. Moreover, we conduct Welch’s t-test with a significance level of 0.05. We highlight the highest performance in bold. In cases where statistical significance is not observed, we underline all other results within the significance level.

Models. We use LLaVA-1.5-7B (Liu et al., 2024b) and Qwen-VL-2.5-7B (Bai et al., 2025) as MLLMs. During training, we update only the LoRA adapters (Hu et al., 2022), keeping the LLM

Method	Selection Ratio (%)					
	6.25		12.5		25.0	
	$A_{avg} \uparrow$	$A_{last} \uparrow$	$A_{avg} \uparrow$	$A_{last} \uparrow$	$A_{avg} \uparrow$	$A_{last} \uparrow$
Full-Data Training	71.80±0.44	79.66±0.43	71.80±0.44	79.66±0.43	71.80±0.44	79.66±0.43
Random	61.15±0.34	67.29±0.61	64.50±0.22	71.33±0.47	65.48±0.73	73.84±0.45
GradNorm (ICML 2018)	61.23±0.83	66.33±0.73	63.68±1.39	70.51±0.10	<u>65.81±1.37</u>	72.03±0.94
Self-Sup (NeurIPS 2022)	58.05±0.77	64.61±1.16	62.84±0.73	69.48±0.62	64.39±1.26	71.81±0.13
COINCIDE (EMNLP 2024)	59.28±1.45	64.83±0.45	62.33±0.92	69.50±0.39	64.92±0.81	72.25±1.17
DBP (ICLR 2024)	57.14±0.51	63.24±0.82	60.64±1.06	67.85±1.19	62.14±1.42	70.13±1.39
InfoBatch (ICLR 2024)	60.82±0.75	68.88±1.09	64.87±0.68	73.63±0.28	<u>66.41±1.36</u>	74.70±0.52
DivBS (ICML 2024)	61.07±0.58	69.06±0.54	65.31±0.41	<u>73.76±0.85</u>	<u>64.22±0.71</u>	<u>75.38±1.25</u>
TIVE (arXiv:2403)	58.75±1.20	64.19±1.40	61.27±0.59	68.38±0.41	64.29±1.02	72.76±0.83
Adapt-∞ (ICLR 2025)	59.13±0.32	64.37±0.85	61.53±0.84	69.82±0.99	65.50±0.52	73.57±1.22
OASIS (Ours)	64.39±0.58	71.76±0.72	66.89±0.68	75.60±0.26	68.84±0.37	77.95±0.93

Table 1: **Quantitative comparison between sample selection methods on MICVIT benchmark.** LLaVA-1.5-7B is used as the MLLM. Bold indicates the highest performance; underlined results are within the 0.05 t-test significance level. 'Full-Data Training' uses all data without selection.

frozen for training efficiency, following (Ye et al., 2023; Seo et al., 2025).

Baselines. We adopt recent state-of-the-art (SOTA) sample selection methods as baselines: GradNorm (Katharopoulos and Fleuret, 2018), Self-Sup (Sorscher et al., 2022), COINCIDE (Lee et al., 2024), DBP (Abbas et al., 2024), InfoBatch (Qin et al., 2024), DivBS (Hong et al., 2024), TIVE (Liu et al., 2024c), Adapt-∞ (Maharana et al., 2025), and Random selection, which often demonstrates more robustness and stability than the SOTA selection methods (Gupta et al., 2023; Zheng et al., 2023), despite its simplicity. While baselines select a fixed number of samples per batch, OASIS dynamically selects samples probabilistically. For fair comparison, we ensure our approach uses comparable or fewer total samples, as detailed in Sec. A.14. See Sec. A.4 for the baselines' details.

Metrics. We report A_{last} , the accuracy measured at the end of training, and A_{avg} , the average accuracy measured at each task boundary.

Benchmarks. We conduct experiments on various CVIT benchmarks, including the widely used COAST (Cao et al., 2024) (COAST-domain) and Adapt (Maharana et al., 2025). COAST's key limitation is assuming balanced tasks (*i.e.*, 20,000 samples per task), contradicting real-world imbalanced distributions. Adapt's limitation is including datasets that use COCO (Lin et al., 2014) images, *e.g.*, LaMM (Yin et al., 2023) and M3IT (Li et al., 2023a), which overlap with LLaVA pre-training data. To mitigate issues in COAST and Adapt, we propose Multi-image Imbalanced Continual Visual

Method	Benchmark			
	COAST		Adapt	
	$A_{avg} \uparrow$	$A_{last} \uparrow$	$A_{avg} \uparrow$	$A_{last} \uparrow$
Full-Data Training	31.56±1.42	39.06±0.55	55.89±0.20	54.26±0.23
Random	23.57±0.17	30.80±0.30	47.64±0.21	40.26±0.71
GradNorm (ICML 2018)	21.91±0.47	28.08±0.49	44.92±0.06	36.78±0.52
Self-Sup (NeurIPS 2022)	22.16±0.27	30.09±0.51	43.85±0.75	34.49±1.37
COINCIDE (EMNLP 2024)	22.56±0.90	29.89±1.42	44.56±0.84	35.83±0.48
DBP (ICLR 2024)	20.28±0.81	28.67±0.32	43.25±0.45	34.75±0.54
InfoBatch (ICLR 2024)	22.93±0.73	29.14±0.56	47.65±0.30	40.60±0.96
DivBS (ICML 2024)	23.41±0.14	31.72±0.18	47.25±0.74	40.38±0.62
TIVE (arXiv:2403)	21.15±0.09	28.12±0.10	44.72±0.58	35.28±1.37
Adapt-∞ (ICLR 2025)	22.42±0.16	29.39±0.72	45.06±0.34	35.51±1.29
OASIS (Ours)	25.67±0.35	34.23±0.38	49.98±0.27	43.94±0.31

Table 2: **Quantitative comparison on COAST and Adapt under selection ratio 6.25%.** We use LLaVA-1.5-7B as an MLLM. 'Full-Data Training' uses all data without selection.

Instruction Tuning (MICVIT), which excludes data from LLaVA and Qwen-VL pretraining while preserving the imbalanced distribution as in real-world scenarios. MICVIT comprises NLVR2 (Suhr et al., 2017), Bongard-OpenWorld (Wu et al., 2024b), Bongard-HOI (Jiang et al., 2022), Co-Instruct-DB (Wu et al., 2024a), DVQA (Kafle et al., 2018), HQ-Edit (Hui et al., 2025), and Pattern-Com (Psomas et al., 2024). To reflect real-world complexity, we mostly adopt multi-image data, except for Co-Instruct-DB and DVQA.

More details on implementation and benchmarks can be found in Sec. A.1 and A.3, respectively.

4.2 Quantitative Analysis

Comparison across Various Sample Selection Ratios. We compare OASIS with the baselines by training LLaVA-1.5-7B on MICVIT under various sample selection ratios (*i.e.*, 6.25%, 12.5%, and

Method	Selection Ratio (%)			
	6.25		12.5	
	$A_{avg} \uparrow$	$A_{last} \uparrow$	$A_{avg} \uparrow$	$A_{last} \uparrow$
Full-Data Training	72.31±0.42	78.18±0.75	72.31±0.42	78.18±0.75
Random	59.23±0.85	65.94±0.38	62.18±0.19	69.03±0.10
GradNorm (ICML 2018)	57.49±0.92	63.38±0.64	63.90±0.22	69.34±0.47
Self-Sup (NeurIPS 2022)	54.29±0.56	61.42±0.31	61.37±0.99	68.32±0.38
COINCIDE (EMNLP 2024)	57.34±0.77	62.90±0.48	62.38±0.73	69.23±0.44
DBP (ICLR 2024)	54.53±0.43	60.38±0.56	60.63±0.30	67.81±0.52
InfoBatch (ICLR 2024)	58.14±0.28	65.38±0.87	64.04±0.42	68.26±1.31
DivBS (ICLR 2024)	<u>60.28±0.98</u>	67.48±0.29	<u>65.26±1.34</u>	70.48±0.38
TIVE (arXiv:2403)	55.84±0.49	63.37±0.83	62.11±0.45	67.42±0.73
Adapt-∞ (ICLR 2025)	56.32±0.97	62.48±0.38	62.35±0.49	67.82±1.24
OASIS (Ours)	61.64±0.43	69.43±0.72	66.54±0.88	72.35±0.28

Table 3: **Quantitative comparison on MICVIT benchmark.** We use Qwen-VL-2.5-7B as the MLLM. Bold indicates the highest performance; underlined results are within the 0.05 t-test significance level. 'Full-Data Training' uses all data without selection.

25.0%), and summarize the results in Tab. 1. As shown in the table, OASIS outperforms baselines by significant margins. Specifically, the gap between OASIS and the baselines is particularly large at the lowest sample selection ratio, *i.e.*, 6.25%.

Since each individual data point has more influence on smaller coreset sizes (Zheng et al., 2023; Jafari et al., 2024), this result further demonstrates the effectiveness of our method in selecting informative data. Moreover, with 25.0% selection ratio, OASIS achieves performance comparable to Full-Data Training, with only an approximately 1%–2% drop in A_{last} on both MICVIT. Furthermore, improvements in both A_{last} and A_{avg} shows that OASIS not only enhances final performance but also accelerates convergence by prioritizing informative samples.

Comparison across Various Benchmarks. We also compare OASIS with baselines on existing CVIT benchmarks, *i.e.*, COAST and Adapt, under selection ratio 6.25% in Tab. 2. OASIS consistently outperforms across both COAST and Adapt, demonstrating its robustness across benchmarks. We provide additional results with various selection ratios on COAST and Adapt in Sec. A.2

Comparison in Qwen-VL-2.5 Training. We then evaluate OASIS in training Qwen-VL-2.5-7B, and summarize the results in Tab. 3. Consistent with the results observed in LLaVA training (Tab. 1), OASIS significantly outperforms baselines across various sample selection ratios. These findings demonstrate that the samples selected by OASIS consistently enhance training efficiency, regardless of the underlying model architecture. We provide additional results of Qwen-VL-2.5 training on the COAST and Adapt benchmarks in Sec. A.5.

Comparison of Computation Budget. We com-

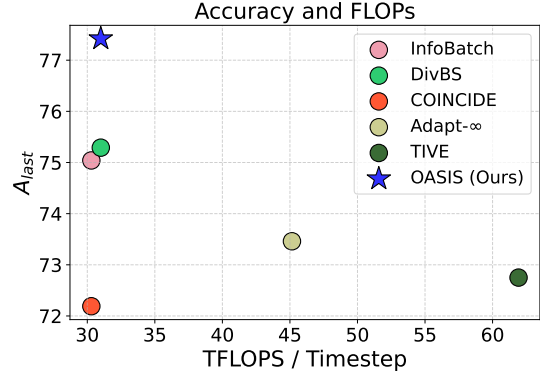


Figure 4: **Accuracy and FLOPs with 25% selection ratio on MICVIT.** The top-left corner illustrates effective and efficient sample selection.

pare the computational cost of OASIS with baselines and summarize the results in Fig. 4 on MICVIT. As shown in the figure, OASIS outperforms baselines and achieves comparable accuracy with full-data training, while consuming fewer FLOPs. We provide a more detailed computational analysis of each method in Sec. A.11.

Comparison of Selected Samples' Diversity. We assess the diversity of samples selected by each method by computing their densities through measuring the mean pairwise distance in a Gaussian kernel, following (Lee et al., 2024). As shown in Tab. 4, selected samples with OASIS achieve the highest diversity compared to baselines. We believe the probabilistic selection in OASIS enhances the diversity of selected samples, while SIREN effectively reduces redundancy among them.

Method	MICVIT	COAST
Random	0.263	0.624
GradNorm (ICML 2018)	0.255	0.598
Self-Sup (NeurIPS 2022)	0.358	0.581
COINCIDE (EMNLP 2024)	0.259	0.604
DBP (ICLR 2024)	0.288	0.587
InfoBatch (ICLR 2024)	0.308	0.632
DivBS (ICML 2024)	0.291	0.625
Adapt-∞ (ICLR 2025)	0.274	0.578
OASIS (Ours)	0.242	0.563

Table 4: **Density comparison of selected samples.** Lower density indicates higher diversity.

Comparison of Fast Adaptation Performance.

We compare the fast adaptation performance across various unseen downstream tasks after CVIT, with CVIT serving as the upstream continual pre-training. This comparison evaluates the generalizability of models trained with samples selected by each online sample selection method. We consider COMICS (Iyyer et al., 2017), VISION (Bai

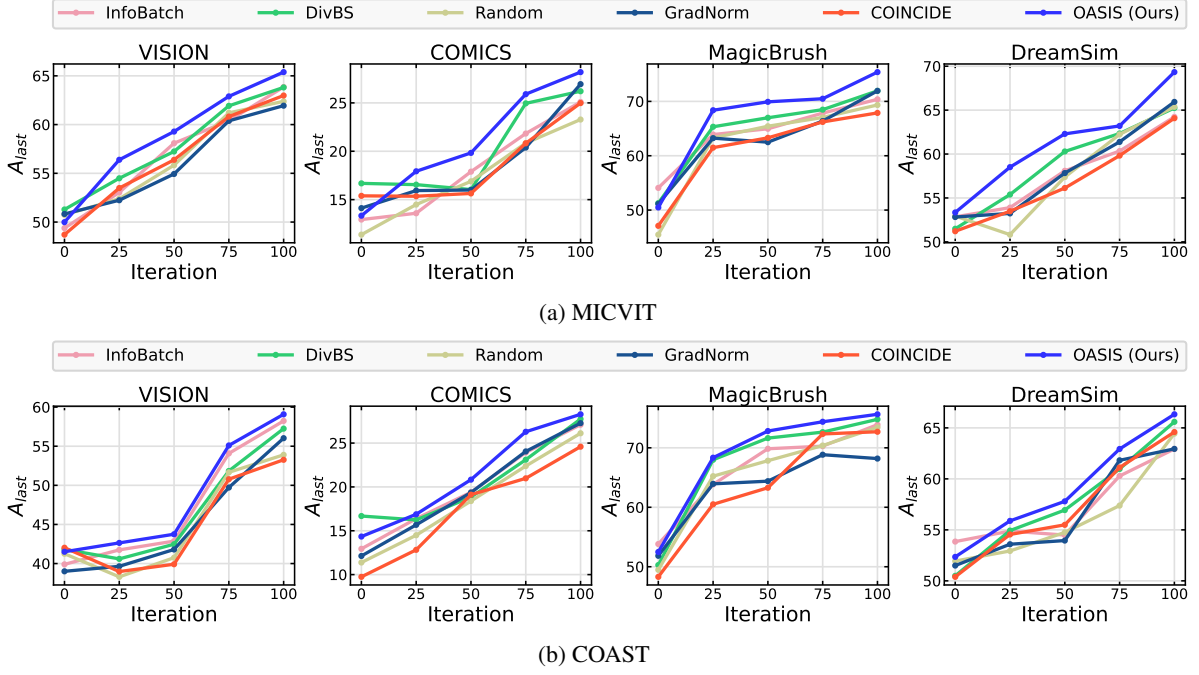


Figure 5: **Comparison of fast adaptation performance.** After CVIT of LLaVA-1.5-7B on subsets (25% of the full data), selected using each sample selection baseline from (a) MICVIT and (b) COAST, we fine-tune the model for 100 epochs on each downstream task (*i.e.*, VISION, COMICS, MagicBrush, and DreamSim).

et al., 2023a), DreamSim (Fu et al., 2023), and Magicbrush (Zhang et al., 2023) as downstream tasks. We use MICVIT and COAST as upstream tasks, and summarize the results in Fig. 5. As shown in the figure, the model trained on the subset selected by OASIS consistently outperforms all baselines, demonstrating superior generalizability. Note that the performance at iteration 0 (*i.e.*, zero-shot performance) can vary depending on the similarity between the downstream tasks and the subset of data selected by each baseline, resulting in inconsistent ordering between baselines. However, as training on downstream tasks progresses, we observe that OASIS consistently achieves faster adaptation compared to baselines, demonstrating the superior generalizability of models trained on subsets selected by OASIS.

4.3 Ablation Study

Ablation Study on Different Components. We ablate OASIS to investigate the benefit of each proposed component, and summarize the results in Tab. 5. As shown, ORIS significantly improves performance by identifying informative samples, while SIREN further enhances performance by reducing redundancy between selected samples. Consistent improvements across benchmarks validate the effectiveness of our proposed components.

Additional Analyses. We provide additional anal-

Method	MICVIT		COAST	
	$A_{avg} \uparrow$	$A_{last} \uparrow$	$A_{avg} \uparrow$	$A_{last} \uparrow$
Vanilla	59.82 \pm 0.73	64.34 \pm 1.25	20.45 \pm 0.67	27.17 \pm 0.29
(+) ORIS	63.04 \pm 0.48	69.72 \pm 0.45	24.87 \pm 1.33	33.51 \pm 0.81
(+) ORIS & SIREN (Ours)	64.39\pm0.58	71.76\pm0.72	25.67\pm0.35	34.23\pm0.38

Table 5: **Ablations for proposed components of OASIS on MICVIT and COAST.** We train LLaVA-1.5-7B with 6.25% of samples selected from the entire dataset. Vanilla: selecting a fixed number of samples with the highest Fisher Information within each batch.

yses, including informativeness metric evaluations (Sec. A.7), effect of task orders (Sec. A.8), effect of EMA ratio α (Sec. A.9), accuracy over time in CVIT (Sec. A.10), computational cost comparisons (Sec. A.11), and comparison of the number of selected samples (Sec. A.14).

5 Conclusion

We address the challenge of achieving high performance while training on a small subset of data in the online CVIT setup. Prior works select a fixed number of samples per batch, which struggles in the CVIT setup due to varying informativeness and frequent redundancy from co-occurring similar samples. To address this, we propose OASIS, comprising two components: Online Relative Informativeness Selection (ORIS), which adaptively selects samples based on relative informativeness, and Similarity-aware Information Redundancy Elim-

ination (SIREN), which reduces redundancy via sample-wise similarity. Extensive experiments on diverse CVIT benchmarks demonstrate that our proposed OASIS consistently selects informative samples, outperforms existing baselines, and achieves performance comparable to full-data training.

Limitations

Requiring only a single forward pass, our method efficiently estimates informativeness measures for online samples in CVIT. A promising direction for future work is to further eliminate the need for forward passes altogether when estimating informativeness, potentially enabling near-instantaneous adaptation and significantly faster processing in real-time applications for CVIT.

Acknowledgment

This work was partly supported by IITP grants funded by the Korean government (MSIT): No. RS-2022-II220077, RS-2022-II220113, RS-2022-II220959, RS-2022-II220871, RS-2022-II220951 (50%), RS-2021-II211343 (SNU AI), and RS-2021-II212068 (AI Innovation Hub). Additional support was provided by the BK21 FOUR program, SNU in 2025, and the European Research Council (ERC-2020-AdG 101021347, KeepOnLearning).

References

- Amro Abbas, Evgenia Rusak, Kushal Tirumala, Wieland Brendel, Kamalika Chaudhuri, and Ari S Morcos. 2024. Effective pruning of web-scale datasets based on complexity of concept clusters. *arXiv preprint arXiv:2401.04578*.
- Amro Abbas, Kushal Tirumala, Dániel Simig, Surya Ganguli, and Ari S Morcos. 2023. Semdedup: Data-efficient learning at web-scale through semantic deduplication. *arXiv preprint arXiv:2303.09540*.
- Haoping Bai, Shancong Mou, Tatiana Likhomanenko, Ramazan Gokberk Cinbis, Oncel Tuzel, Ping Huang, Jiulong Shan, Jianjun Shi, and Meng Cao. 2023a. Vision datasets: A benchmark for vision-based industrial inspection. *arXiv preprint arXiv:2306.07890*.
- Jinze Bai, Shuai Bai, Yunfei Chu, Zeyu Cui, Kai Dang, Xiaodong Deng, Yang Fan, Wenbin Ge, Yu Han, Fei Huang, and 1 others. 2023b. Qwen technical report. *arXiv preprint arXiv:2309.16609*.
- Shuai Bai, Keqin Chen, Xuejing Liu, Jialin Wang, Wenbin Ge, Sibao Song, Kai Dang, Peng Wang, Shijie Wang, Jun Tang, and 1 others. 2025. Qwen2. 5-vl technical report. *arXiv preprint arXiv:2502.13923*.
- Jihwan Bang, Heesu Kim, YoungJoon Yoo, Jung-Woo Ha, and Jonghyun Choi. 2021. Rainbow memory: Continual learning with a memory of diverse samples. In *CVPR*.
- Lucas Caccia, Jing Xu, Myle Ott, Marcaurelio Ranzato, and Ludovic Denoyer. 2022. On anytime learning at macroscale. In *CoLLAs*. PMLR.
- Meng Cao, Yuyang Liu, Yingfei Liu, Tiancai Wang, Jiahua Dong, Henghui Ding, Xiangyu Zhang, Ian Reid, and Xiaodan Liang. 2024. Continual llava: Continual instruction tuning in large vision-language models. *arXiv preprint arXiv:2411.02564*.
- Cheng Chen, Junchen Zhu, Xu Luo, Hengtao Shen, Jingkuan Song, and Lianli Gao. 2024a. Coin: A benchmark of continual instruction tuning for multi-model large language models. In *NeurIPS*.
- Haokun Chen, Yao Zhang, Denis Krompass, Jindong Gu, and Volker Tresp. 2024b. Feddat: An approach for foundation model finetuning in multi-modal heterogeneous federated learning. In *AAAI*, volume 38, pages 11285–11293.
- Jinpeng Chen, Runmin Cong, Yuzhi Zhao, Hongzheng Yang, Guangneng Hu, Horace Ho Shing Ip, and Sam Kwong. 2025. Sefe: Superficial and essential forgetting eliminator for multimodal continual instruction tuning. *arXiv preprint arXiv:2505.02486*.
- Keqin Chen, Zhao Zhang, Weili Zeng, Richong Zhang, Feng Zhu, and Rui Zhao. 2023. Shikra: Unleashing multimodal llm’s referential dialogue magic. *arXiv preprint arXiv:2306.15195*.
- Hsiang-Yun Sherry Chien, Javier S Turek, Nicole Beckage, Vy A Vo, Christopher J Honey, and Ted L Willke. 2021. Slower is better: revisiting the forgetting mechanism in lstm for slower information decay. *arXiv preprint arXiv:2105.05944*.
- Cody Coleman, Christopher Yeh, Stephen Mussmann, Baharan Mirzasoleiman, Peter Bailis, Percy Liang, Jure Leskovec, and Matei Zaharia. 2019. Selection via proxy: Efficient data selection for deep learning. *arXiv preprint arXiv:1906.11829*.
- Cody Coleman, Christopher Yeh, Stephen Mussmann, Baharan Mirzasoleiman, Peter Bailis, Percy Liang, Jure Leskovec, and Matei Zaharia. 2020. Selection via proxy: Efficient data selection for deep learning. In *ICLR*.
- Danruo Deng, Guangyong Chen, Yang Yu, Furui Liu, and Pheng-Ann Heng. 2023a. Uncertainty estimation by fisher information-based evidential deep learning. In *ICML*. PMLR.
- Zhiqiang Deng, Peng Cui, and Jun Zhu. 2023b. Towards accelerated model training via bayesian data selection. In *NeurIPS*.

- Yunshu Du, Wojciech M Czarnecki, Siddhant M Jayakumar, Mehrdad Farajtabar, Razvan Pascanu, and Balaji Lakshminarayanan. 2018. Adapting auxiliary losses using gradient similarity. *arXiv preprint arXiv:1812.02224*.
- Stephanie Fu, Netanel Tamir, Shobhita Sundaram, Lucy Chai, Richard Zhang, Tali Dekel, and Phillip Isola. 2023. Dreamsim: Learning new dimensions of human visual similarity using synthetic data. In *NeurIPS*, volume 36, pages 50742–50768.
- Yasir Ghunaim, Adel Bibi, Kumail Alhamoud, Motasem Alfarra, Hasan Abed Al Kader Hammoud, Ameya Prabhu, Philip HS Torr, and Bernard Ghanem. 2023. Real-time evaluation in online continual learning: A new hope. In *CVPR*.
- Haiyang Guo, Fanhu Zeng, Ziwei Xiang, Fei Zhu, Da-Han Wang, Xu-Yao Zhang, and Cheng-Lin Liu. 2025. Hide-llava: Hierarchical decoupling for continual instruction tuning of multimodal large language model. *arXiv preprint arXiv:2503.12941*.
- Animesh Gupta, Irtiza Hasan, Dilip K Prasad, and Deepak K Gupta. 2023. Data-efficient training of cnns and transformers with coresets: A stability perspective. *arXiv preprint arXiv:2303.02095*.
- Jinghan He, Haiyun Guo, Ming Tang, and Jinqiao Wang. 2023. Continual instruction tuning for large multimodal models. *arXiv preprint arXiv:2311.16206*.
- Xuehai He, Yichen Zhang, Luntian Mou, Eric Xing, and Pengtao Xie. 2020. Pathvqa: 30000+ questions for medical visual question answering. *arXiv preprint arXiv:2003.10286*.
- Aral Hekimoglu, Adrian Brucker, Alper Kagan Kayali, Michael Schmidt, and Alvaro Marcos-Ramiro. 2023. Active learning for object detection with non-redundant informative sampling. *arXiv preprint arXiv:2307.08414*.
- Feng Hong, Yueming Lyu, Jiangchao Yao, Ya Zhang, Ivor W Tsang, and Yanfeng Wang. 2024. Diversified batch selection for training acceleration. *arXiv preprint arXiv:2406.04872*.
- Edward J Hu, Phillip Wallis, Zeyuan Allen-Zhu, Yuanzhi Li, Shean Wang, Lu Wang, Weizhu Chen, and 1 others. 2022. Lora: Low-rank adaptation of large language models. In *ICLR*.
- Mude Hui, Siwei Yang, Bingchen Zhao, Yichun Shi, Heng Wang, Peng Wang, Cihang Xie, and Yuyin Zhou. 2025. HQ-edit: A high-quality dataset for instruction-based image editing. In *ICLR*.
- Zhouyuan Huo, Bin Gu, and Heng Huang. 2018. Training neural networks using features replay.
- Mohit Iyyer, Varun Manjunatha, Anupam Guha, Yogarshi Vyas, Jordan Boyd-Graber, Hal Daume, and Larry S Davis. 2017. The amazing mysteries of the gutter: Drawing inferences between panels in comic book narratives. In *CVPR*, pages 7186–7195.
- Mohammad Jafari, Yimeng Zhang, Yihua Zhang, and Sijia Liu. 2024. The power of few: Accelerating and enhancing data reweighting with coreset selection. In *ICASSP*, pages 7100–7104. IEEE.
- Dongfu Jiang, Xuan He, Huaye Zeng, Cong Wei, Max Ku, Qian Liu, and Wenhui Chen. 2024. Mantis: Interleaved multi-image instruction tuning. *Transactions on Machine Learning Research*.
- Huaizu Jiang, Xiaojuan Ma, Weili Nie, Zhiding Yu, Yuke Zhu, and Anima Anandkumar. 2022. Bongard-hoi: Benchmarking few-shot visual reasoning for human-object interactions. In *CVPR*, pages 19056–19065.
- Kushal Kafle, Brian Price, Scott Cohen, and Christopher Kanan. 2018. Dvqa: Understanding data visualizations via question answering. In *CVPR*, pages 5648–5656.
- Angelos Katharopoulos and François Fleuret. 2018. Not all samples are created equal: Deep learning with importance sampling. In *ICML*, pages 2525–2534. PMLR.
- Been Kim, Rajiv Khanna, and Oluwasanmi O Koyejo. 2016. Examples are not enough, learn to criticize! criticism for interpretability. In *Advances in neural information processing systems*.
- James Kirkpatrick, Razvan Pascanu, Neil Rabinowitz, Joel Veness, Guillaume Desjardins, Andrei A Rusu, Kieran Milan, John Quan, Tiago Ramalho, Agnieszka Grabska-Barwinska, and 1 others. 2017. Overcoming catastrophic forgetting in neural networks. *Proceedings of the national academy of sciences*, 114(13):3521–3526.
- Andreas Kirsch and Yarin Gal. 2022. Unifying approaches in active learning and active sampling via fisher information and information-theoretic quantities. *arXiv preprint arXiv:2208.00549*.
- Hyunseo Koh, Dahyun Kim, Jung-Woo Ha, and Jonghyun Choi. 2022. Online continual learning on class incremental blurry task configuration with anytime inference. In *ICLR*.
- Hyunseo Koh, Minhyuk Seo, Jihwan Bang, Hwanjun Song, Deokki Hong, Seulki Park, Jung-Woo Ha, and Jonghyun Choi. 2023. Online boundary-free continual learning by scheduled data prior. In *ICLR*.
- Kamil Książek, Hubert Jastrzębski, Bartosz Trojan, Krzysztof Pniacsek, Michał Karp, and Jacek Tabor. 2025. Fenec: Enhancing continual learning via feature clustering with neighbor-or logit-based classification. *arXiv preprint arXiv:2503.14301*.
- Allison Lau, Younwoo Choi, Vahid Balazadeh, Keertana Chidambaram, Vasilis Syrgkanis, and Rahul G Krishnan. 2024. Personalized adaptation via in-context preference learning. *arXiv preprint arXiv:2410.14001*.

- Jaewoo Lee, Boyang Li, and Sung Ju Hwang. 2024. Concept-skill transferability-based data selection for large vision-language models. In *EMNLP*.
- Lei Li, Yuwei Yin, Shicheng Li, Liang Chen, Peiyi Wang, Shuhuai Ren, Mukai Li, Yazheng Yang, Jingjing Xu, Xu Sun, and 1 others. 2023a. M³ it: A large-scale dataset towards multi-modal multilingual instruction tuning. *arXiv preprint arXiv:2306.04387*.
- Ming Li, Yong Zhang, Zhitao Li, Jiuai Chen, Lichang Chen, Ning Cheng, Jianzong Wang, Tianyi Zhou, and Jing Xiao. 2023b. From quantity to quality: Boosting llm performance with self-guided data selection for instruction tuning. *arXiv preprint arXiv:2308.12032*.
- Tsung-Yi Lin, Michael Maire, Serge Belongie, James Hays, Pietro Perona, Deva Ramanan, Piotr Dollár, and C Lawrence Zitnick. 2014. Microsoft coco: Common objects in context. In *ECCV*.
- Aixin Liu, Bei Feng, Bing Xue, Bingxuan Wang, Bochao Wu, Chengda Lu, Chenggang Zhao, Chengqi Deng, Chenyu Zhang, Chong Ruan, and 1 others. 2024a. Deepseek-v3 technical report. *arXiv preprint arXiv:2412.19437*.
- Haotian Liu, Chunyuan Li, Yuheng Li, and Yong Jae Lee. 2024b. Improved baselines with visual instruction tuning. In *CVPR*.
- Haotian Liu, Chunyuan Li, Qingyang Wu, and Yong Jae Lee. 2023. Visual instruction tuning.
- Zikang Liu, Kun Zhou, Wayne Xin Zhao, Dawei Gao, Yaliang Li, and Ji-Rong Wen. 2024c. Less is more: High-value data selection for visual instruction tuning. *arXiv preprint arXiv:2403.09559*.
- Pan Lu, Liang Qiu, Jiaqi Chen, Tony Xia, Yizhou Zhao, Wei Zhang, Zhou Yu, Xiaodan Liang, and Song-Chun Zhu. 2021. Iconqa: A new benchmark for abstract diagram understanding and visual language reasoning. In *NeurIPS*.
- Chengcheng Ma, Yang Liu, Jiankang Deng, Lingxi Xie, Weiming Dong, and Changsheng Xu. 2023. Understanding and mitigating overfitting in prompt tuning for vision-language models. *IEEE Transactions on Circuits and Systems for Video Technology*, 33(9):4616–4629.
- Adyasha Maharana, Jaehong Yoon, Tianlong Chen, and Mohit Bansal. 2025. Adapt-\$\infty\$: Scalable continual multimodal instruction tuning via dynamic data selection. In *ICLR*.
- Shivangi Mahto, Vy Ai Vo, Javier S Turek, and Alexander Huth. 2020. Multi-timescale representation learning in lstm language models. In *ICLR*.
- Ahmed Masry, Xuan Long Do, Jia Qing Tan, Shafiq Joty, and Enamul Hoque. 2022. Chartqa: A benchmark for question answering about charts with visual and logical reasoning. In *ACL*, pages 2263–2279.
- Minesh Mathew, Dimosthenis Karatzas, and CV Jawahar. 2021. Docvqa: A dataset for vqa on document images. In *WACV*.
- Sören Mindermann, Jan M Brauner, Muhammed T Razzak, Mrinank Sharma, Andreas Kirsch, Winnie Xu, Benedikt Höltingen, Aidan N Gomez, Adrien Morisot, Sebastian Farquhar, and 1 others. 2022. Prioritized training on points that are learnable, worth learning, and not yet learnt. In *ICML*. PMLR.
- Aristeidis Panos, Rahaf Aljundi, Daniel Olmeda Reino, and Richard E Turner. 2025. Efficient few-shot continual learning in vision-language models. *arXiv preprint arXiv:2502.04098*.
- Mansheej Paul, Surya Ganguli, and Gintare Karolina Dziugaite. 2021. Deep learning on a data diet: Finding important examples early in training. In *NeurIPS*.
- Bill Psomas, Ioannis Kakogeorgiou, Nikos Efthymiadis, Giorgos Tolias, Ondřej Chum, Yannis Avrithis, and Konstantinos Karantzalos. 2024. Composed image retrieval for remote sensing. In *IGARSS*, pages 8526–8534. IEEE.
- Ziheng Qin, Kai Wang, Zangwei Zheng, Jianyang Gu, Xiangyu Peng, Zhaopan Xu, Daquan Zhou, Lei Shang, Baigui Sun, Xuansong Xie, and 1 others. 2024. Infobatch: Lossless training speed up by unbiased dynamic data pruning. In *ICLR*.
- Leslie Rice, Eric Wong, and Zico Kolter. 2020. Overfitting in adversarially robust deep learning. In *ICML*.
- Minhyuk Seo, Seongwon Cho, Minjae Lee, Diganta Misra, Hyeonbeom Choi, Seon Joo Kim, and Jonghyun Choi. 2024a. Just say the name: Online continual learning with category names only via data generation. *arXiv preprint arXiv:2403.10853*.
- Minhyuk Seo, Hyunseo Koh, and Jonghyun Choi. 2025. Budgeted online continual learning by adaptive layer freezing and frequency-based sampling. In *ICLR*.
- Minhyuk Seo, Hyunseo Koh, Wonje Jeung, Minjae Lee, San Kim, Hankook Lee, Sungjun Cho, Sungik Choi, Hyunwoo Kim, and Jonghyun Choi. 2024b. Learning equi-angular representations for online continual learning. In *CVPR*, pages 23933–23942.
- Hyo-Sang Shin and Hae-In Lee. 2020. A new exponential forgetting algorithm for recursive least-squares parameter estimation. *arXiv preprint arXiv:2004.03910*.
- Seungjae Shin, Heesun Bae, Donghyeok Shin, Weonyoung Joo, and Il-Chul Moon. 2023. Loss-curvature matching for dataset selection and condensation. In *AISTATS*. PMLR.
- Alexander Soen and Ke Sun. 2021. On the variance of the fisher information for deep learning. In *NeurIPS*.
- Ben Sorscher, Robert Geirhos, Shashank Shekhar, Surya Ganguli, and Ari Morcos. 2022. Beyond neural scaling laws: beating power law scaling via data pruning. In *NeurIPS*.

- Alane Suhr, Mike Lewis, James Yeh, and Yoav Artzi. 2017. A corpus of natural language for visual reasoning. In *ACL*.
- Ziqi Wang, Chang Che, Qi Wang, Yangyang Li, Zenglin Shi, and Meng Wang. 2024. Separable mixture of low-rank adaptation for continual visual instruction tuning. *arXiv preprint arXiv:2411.13949*.
- Haoning Wu, Hanwei Zhu, Zicheng Zhang, Erli Zhang, Chaofeng Chen, Liang Liao, Chunyi Li, Annan Wang, Wenxiu Sun, Qiong Yan, and 1 others. 2024a. Towards open-ended visual quality comparison. In *ECCV*, pages 360–377. Springer.
- Rujie Wu, Xiaojian Ma, Zhenliang Zhang, Wei Wang, Qing Li, Song-Chun Zhu, and Yizhou Wang. 2024b. Bongard-openworld: Few-shot reasoning for free-form visual concepts in the real world. In *ICLR*.
- Zhiyang Xu, Ying Shen, and Lifu Huang. 2023. Multi-instruct: Improving multi-modal zero-shot learning via instruction tuning. In *ACL*, pages 11445–11465. Association for Computational Linguistics.
- An Yang, Baosong Yang, Beichen Zhang, Binyuan Hui, Bo Zheng, Bowen Yu, Chengyuan Li, Dayiheng Liu, Fei Huang, Haoran Wei, and 1 others. 2024. Qwen2.5 technical report. *arXiv preprint arXiv:2412.15115*.
- Qinghao Ye, Haiyang Xu, Guohai Xu, Jiabo Ye, Ming Yan, Yiyang Zhou, Junyang Wang, Anwen Hu, Pengcheng Shi, Yaya Shi, and 1 others. 2023. mplug-owl: Modularization empowers large language models with multimodality. *arXiv preprint arXiv:2304.14178*.
- Zhenfei Yin, Jiong Wang, Jianjian Cao, Zhelun Shi, Dingning Liu, Mukai Li, Xiaoshui Huang, Zhiyong Wang, Lu Sheng, Lei Bai, and 1 others. 2023. Lamm: Language-assisted multi-modal instruction-tuning dataset, framework, and benchmark. In *NeurIPS*.
- Yuexiang Zhai, Shengbang Tong, Xiao Li, Mu Cai, Qing Qu, Yong Jae Lee, and Yi Ma. 2023. Investigating the catastrophic forgetting in multimodal large language models. *arXiv preprint arXiv:2309.10313*.
- Jiarui Zhang. 2024. Guided profile generation improves personalization with llms. In *ACL*.
- Kai Zhang, Lingbo Mo, Wenhui Chen, Huan Sun, and Yu Su. 2023. Magicbrush: A manually annotated dataset for instruction-guided image editing. In *NeurIPS*. Curran Associates, Inc.
- Haizhong Zheng, Rui Liu, Fan Lai, and Atul Prakash. 2023. Coverage-centric coreset selection for high pruning rates. In *ICLR*.
- Junhao Zheng, Qianli Ma, Zhen Liu, Binqian Wu, and Huawei Feng. 2024. Beyond anti-forgetting: Multimodal continual instruction tuning with positive forward transfer. *arXiv preprint arXiv:2401.09181*.
- Deyao Zhu, Jun Chen, Xiaoqian Shen, Xiang Li, and Mohamed Elhoseiny. 2023. Minigpt-4: Enhancing vision-language understanding with advanced large language models. *arXiv preprint arXiv:2304.10592*.
- Deyao Zhu, Jun Chen, Xiaoqian Shen, Xiang Li, and Mohamed Elhoseiny. 2024. [MiniGPT-4: Enhancing vision-language understanding with advanced large language models](#). In *ICLR*.

A Technical Appendices and Supplementary Material

A.1 Implementation Details

We fine-tune models using learning rates from their original papers for one epoch: $2e-5$ for LLaVA-1.5-7B and $2e-7$ for Qwen-VL-2.5-7B. We use the Adam optimizer with no decay and a Cosine LR scheduler. For batch size N_B , we use 16 for all experiments. For LoRA finetuning, we adopt LoRA with rank 128 at all linear layers in the LLM backbone. We set the number of batch iterations per sample encounter to COAST, Adapt, and MICVIT as 0.125, 0.125, and 0.0625, respectively. We assume an infinite memory setup, which assumes that all encountered samples can be stored in an episodic memory. For the batch retrieval method, we adopt memory-only training (Koh et al., 2022; Seo et al., 2024b), where training batches are only retrieved from the episodic memory at each iteration, enhancing robustness to distribution shifts (Koh et al., 2023; Seo et al., 2025). We set the EMA ratio α to 0.9 for all datasets. We conduct experiments on NVIDIA RTX A6000 GPUs. Every experiment takes no more than 1.5 days.

A.2 Experimental Results on Various Benchmarks

In addition to MICVIT, we compare OASIS with sample selection methods in COAST (Cao et al., 2024) and Adapt (Maharana et al., 2025) under selection ratio 12.5% and 25.0% in Tab. 6 and Tab. 7, respectively. OASIS not only outperforms selection baselines but also shows comparable results with a model trained on all data (*i.e.*, Full-Data Training) in diverse benchmarks.

Method	Benchmark			
	COAST		Adapt	
	$A_{avg} \uparrow$	$A_{last} \uparrow$	$A_{avg} \uparrow$	$A_{last} \uparrow$
Full-Data Training	31.56±1.42	39.06±0.55	55.89±0.20	54.26±0.23
Random	24.58±0.17	32.45±0.92	49.04±0.49	44.19±0.62
GradNorm (ICML 2018)	23.35±0.38	29.44±0.28	48.47±0.63	45.36±0.62
Self-Sup (NeurIPS 2022)	23.72±0.27	31.37±0.75	47.04±0.26	43.94±1.38
COINCIDE (EMNLP 2024)	24.45±0.84	31.08±0.59	48.52±0.55	44.76±0.43
DBP (ICLR 2024)	22.87±0.33	25.81±0.37	46.24±0.36	43.30±1.08
InfoBatch (ICLR 2024)	24.78±0.58	31.74±0.62	49.77±0.82	47.54±0.36
DivBS (ICML 2024)	25.13±0.12	33.30±0.87	49.96±0.48	47.17±0.51
TIVE (arXiv:2403)	23.41±0.23	30.17±0.43	47.75±0.73	44.38±0.99
Adapt-∞ (ICLR 2025)	24.73±0.36	31.69±0.35	48.38±0.20	45.42±0.46
OASIS (Ours)	27.13±0.70	35.42±0.49	51.73±0.33	49.02±0.85

Table 6: **Quantitative comparison on COAST and Adapt under selection ratio 12.5%**. LLaVA-1.5-7B is used as the MLLM. Bold indicates the highest performance; underlined results are within the 0.05 t-test significance level. ‘Full-Data Training’ uses all data without selection.

Method	Benchmark			
	COAST		Adapt	
	$A_{avg} \uparrow$	$A_{last} \uparrow$	$A_{avg} \uparrow$	$A_{last} \uparrow$
Full-Data Training	31.56±1.42	39.06±0.55	55.89±0.20	54.26±0.23
Random	25.82±0.10	34.28±0.28	50.68±0.30	47.58±0.34
GradNorm (ICML 2018)	25.67±0.21	32.85±0.36	51.29±0.54	48.96±0.81
Self-Sup (NeurIPS 2022)	25.17±0.37	32.84±0.42	49.34±0.85	46.46±0.47
COINCIDE (EMNLP 2024)	26.22±0.34	34.90±0.57	51.74±0.64	47.40±0.31
DBP (ICLR 2024)	24.74±0.70	32.13±0.64	48.58±0.43	45.65±0.84
InfoBatch (ICLR 2024)	25.30±0.35	34.49±0.45	51.55±0.47	49.04±0.77
DivBS (ICML 2024)	26.91±0.02	35.01±0.16	52.36±0.05	50.02±0.21
TIVE (arXiv:2403)	25.18±0.78	34.08±0.60	49.69±1.24	45.97±0.88
Adapt-∞ (ICLR 2025)	26.07±0.25	33.50±0.04	50.56±0.25	47.54±0.53
OASIS (Ours)	28.72±0.63	37.55±0.28	54.58±0.14	51.87±0.49

Table 7: **Quantitative comparison on COAST and Adapt under selection ratio 25.0%**. LLaVA-1.5-7B is used as the MLLM. Bold indicates the highest performance; underlined results are within the 0.05 t-test significance level. ‘Full-Data Training’ uses all data without selection.

A.3 Benchmark Configuration Details

For COAST benchmark, we use the COAST-domain, which emulates a scenario where MLLMs needs to continuously adapt to diverse domains. Specifically, it consists of DocVQA (Mathew et al., 2021), ChartQA (Masry et al., 2022), IconQA (Lu et al., 2021), and MedicalQA (He et al., 2020), which correspond to the document, chart, icon, and medical domains, respectively. Adapt benchmark consists of visual instruction tuning datasets, such as M3IT (Li et al., 2023a), MiniGPT4 (Zhu et al., 2023), MANTIS (Jiang et al., 2024), LaMM (Yin et al., 2023), and VisionFLAN (Xu et al., 2023). We summarize the task configuration of each benchmark including MICVIT in Tab. 8.

A.4 Sample Selection Baselines

Self-Sup (Sorscher et al., 2022). Self-Sup performs K-means clustering on the output embeddings from the final layer of the pretrained model and selects the samples closest to each cluster centroid. By doing so, the most representative sample in the underlying data distribution can be selected.

GradNorm (Katharopoulos and Fleuret, 2018). GradNorm is an importance sampling method that prioritizes the selection of highly informative samples based on gradient magnitude. It computes each sample’s gradient norm with respect to the model’s last layer parameters and assigns higher selection probabilities to samples with larger gradient norms.

COINCIDE (Lee et al., 2024). COINCIDE leverages multi-layer output representations for K-means clustering. Specifically, features are extracted from five distinct layers of the MLLM to

Dataset	# of samples / task	# of tasks	Task order
COAST (Cao et al., 2024)	20,000	4	ChartQA → DocVQA → IconQA → MedicalQA
Adapt (Maharana et al., 2025)	80,000	4	M3IT → MANTIS → LaMM → VisionFLAN
MICVIT (Ours)	50K / 30K / 100K / 46K / 17K / 25K / 79K	7	Bongard-OpenWorld → NLVR2 → Co-Instruct-DB → Bongard-HOI PatternCom → DVQA → HQ Edit

Table 8: Task configurations of CVIT benchmarks.

obtain the representation of the candidate samples. Then it applies K-means clustering to these features, and computes transferability and density metrics of each cluster to determine how many samples should be selected from the respective cluster. Finally, within each cluster, the maximum mean discrepancy (MMD) (Kim et al., 2016) is computed greedily to obtain the samples that best reflect the overall cluster distribution.

DBP (Abbas et al., 2024). DBP aims to improve dataset quality by removing redundant and irrelevant samples. First, following Semdedup (Abbas et al., 2023), DBP applies K-means clustering to group similar samples with last layer outputs and eliminate semantic duplicates by retaining only the sample farthest from the cluster centroid among highly similar pairs. Next, DBP performs CLIP score filtering, removing samples with low text-image similarities. Then, to prioritize more informative data, each cluster is evaluated for its complexity using two metrics: d_{inter} , the distance from the cluster centroid to other centroids, and d_{intra} , the average cosine distance of samples to their own centroid. A complexity score $C_j = d_{\text{inter},j} \cdot d_{\text{intra},j}$ is calculated for each cluster j , and samples are selected proportionally based on this score. Within each selected cluster, samples with the highest entropy are retained, ensuring that the final dataset is both diverse and rich in information.

InfoBatch (Qin et al., 2024). InfoBatch introduces a soft pruning strategy to improve training efficiency while preserving learning dynamics. Unlike traditional hard pruning methods that permanently discard data and risk introducing bias, InfoBatch probabilistically excludes a subset of well-learned samples—identified by their low loss values—during each training epoch. Furthermore, to maintain the integrity of the training trajectory, the gradients of the remaining samples are rescaled such that the expected aggregated gradient approximates that of the full batch.

DivBS (Abbas et al., 2024). From each online batch, DivBS focuses on selecting a fixed subset of

training data that is both informative and diverse by maximizing the orthogonalized representativeness. To do so, DivBS utilizes the last layer gradient. DivBS aims to explicitly reduce inter-sample redundancy, ensuring the retained samples capture complementary and non-overlapping aspects of the batch distribution.

TIVE (Liu et al., 2024c). TIVE selects samples based on two criteria: instance influence and task difficulty, both derived from gradients computed across all layers of a reference model. Instance influence quantifies how much a given sample contributes to other samples during training, while task difficulty estimates the inherent complexity of learning a given task. Guided by these two metrics, TIVE prioritizes samples that are both highly influential and associated with difficult tasks.

Adapt- ∞ (Maharana et al., 2025). Rather than utilizing layer output representations, Adapt- ∞ uses gradients from the middle layer to cluster data into pseudo-tasks, enabling the model to identify and group related skills without requiring explicit task labels. It then performs multi-way sample selection within each cluster using a pool of scoring functions—such as entropy and the proposed Image Grounding score—to retain the most informative samples. Unlike our online continual instruction tuning setting, Adapt- ∞ was introduced in an offline continual instruction tuning setting, where task boundary assumptions exist, limiting its real-world applicability.

A.5 Experiments with Qwen-VL-2.5

In addition to experiments with LLaVA-1.5-7B (Liu et al., 2024b) in Sec. 4.2, we also compare OASIS with sample selection baselines using Qwen-VL-2.5-7B (Bai et al., 2025) as the MLLM. Specifically, we compare OASIS with baselines on COAST, Adapt, and MICVIT, and summarize the results in Tab. 9, Tab. 10, and Tab. 11, respectively. As shown in the tables, OASIS outperforms the baselines, consistent with the results observed using LLaVA-1.5-7B.

Method	Selection Ratio (%)					
	6.25		12.5		25.0	
	$A_{avg} \uparrow$	$A_{last} \uparrow$	$A_{avg} \uparrow$	$A_{last} \uparrow$	$A_{avg} \uparrow$	$A_{last} \uparrow$
Full-Data Training	34.59±0.44	41.90±0.48	34.59±0.44	41.90±0.48	34.59±0.44	41.90±0.48
Random	24.53±0.47	31.59±0.26	26.39±0.54	34.14±0.55	27.89±0.15	37.32±0.28
GradNorm (ICML 2018)	23.85±0.39	29.69±0.84	25.96±0.57	33.28±0.82	26.47±0.19	35.13±1.14
Self-Sup (NeurIPS 2022)	22.44±0.18	30.28±0.80	24.18±1.26	32.53±0.42	25.81±0.05	33.92±0.59
COINCIDE (EMNLP 2024)	21.93±0.45	30.73±0.16	24.74±0.74	33.84±0.43	27.48±0.57	35.27±0.65
DBP (ICLR 2024)	22.58±0.29	27.92±0.27	24.01±0.48	32.43±0.58	25.35±0.52	34.79±0.61
InfoBatch (ICLR 2024)	24.60±0.36	32.88±0.54	27.48±0.39	34.26±1.39	28.93±0.41	38.12±0.42
DivBS (ICML 2024)	25.45±0.64	33.18±0.51	28.29±0.48	<u>36.08±0.85</u>	30.82±0.28	39.87±0.74
TIVE (arXiv:2403)	22.52±0.82	28.90±0.33	25.83±0.62	32.35±0.93	27.14±0.45	34.42±0.14
Adapt-∞ (ICLR 2025)	23.84±0.53	29.48±0.29	24.85±0.84	33.43±0.79	26.78±0.63	35.38±0.38
OASIS (Ours)	27.29±0.18	35.68±0.62	29.16±0.13	36.27±0.75	31.04±0.38	<u>39.38±0.84</u>

Table 9: **Quantitative comparison between online sample selection methods on COAST benchmark.** We use Qwen-VL-2.5-7B as the MLLM. Bold indicates the highest performance; underlined results are within the 0.05 t-test significance level. 'Full-Data Training' uses all data without selection.

Method	Selection Ratio (%)					
	6.25		12.5		25.0	
	$A_{avg} \uparrow$	$A_{last} \uparrow$	$A_{avg} \uparrow$	$A_{last} \uparrow$	$A_{avg} \uparrow$	$A_{last} \uparrow$
Full-Data Training	45.73±1.68	43.92±0.85	45.73±1.68	43.92±0.85	45.73±1.68	43.92±0.85
Random	34.87±0.50	27.49±0.25	36.02±0.35	32.16±0.62	38.73±0.44	34.14±0.57
GradNorm (ICML 2018)	32.53±0.36	25.41±0.72	34.70±0.28	30.25±0.43	35.38±0.40	32.26±0.42
Self-Sup (NeurIPS 2022)	30.31±0.31	22.04±0.65	31.11±0.64	27.73±0.83	33.86±0.50	31.63±1.35
COINCIDE (EMNLP 2024)	32.76±0.17	24.39±0.31	33.93±0.72	29.34±0.47	35.82±0.08	32.38±0.55
DBP (ICLR 2024)	29.82±0.52	22.26±0.36	31.16±0.27	28.04±0.14	34.24±0.61	30.05±0.72
InfoBatch (ICLR 2024)	34.95±0.20	27.19±0.18	35.46±0.83	30.77±0.54	38.25±0.72	34.10±0.50
DivBS (ICML 2024)	34.24±0.75	28.63±0.91	37.24±0.41	31.68±1.39	<u>40.32±0.53</u>	<u>36.59±1.08</u>
TIVE (arXiv:2403)	31.46±0.69	23.74±0.87	32.05±0.06	28.13±0.28	35.49±0.69	31.90±0.35
Adapt-∞ (ICLR 2025)	33.61±0.83	24.93±0.42	34.00±0.57	28.51±1.54	35.36±0.82	32.37±0.63
OASIS (Ours)	36.04±0.26	30.78±0.84	38.72±0.62	33.10±0.43	41.13±0.91	37.36±0.55

Table 10: **Quantitative comparison between online sample selection methods on Adapt benchmark.** We use Qwen-VL-2.5-7B as the MLLM. Bold indicates the highest performance; underlined results are within the 0.05 t-test significance level. 'Full-Data Training' uses all data without selection.

A.6 Details on Determining I_T

As described in Sec. 3.3, we probabilistically select a sample based on its relative informativeness \hat{I} , with the selection probability defined as:

$$p(\hat{I}) = \sigma(\hat{I} - I_T), \quad (9)$$

where $\sigma(\cdot)$ denotes the sigmoid function and I_T is a predefined threshold. We assume $\hat{I} \sim \mathcal{N}(0, 1)$, as we have shown in Fig. 3 that the original (*i.e.*, pre-normalized) informativeness I approximately follows a normal distribution. Based on this normal distribution assumption, the expected selection rate

across the distribution is:

$$f(I_T) = \mathbb{E}_{\hat{I} \sim \mathcal{N}(0,1)}[\sigma(\hat{I} - I_T)] \quad (10)$$

$$= \int_{-\infty}^{\infty} \sigma(\hat{I} - I_T) \cdot \phi(\hat{I}) d\hat{I}, \quad (11)$$

where $\phi(z)$ denotes the standard normal probability density function.

Given target selection rate $r \in [0, 1]$ (*e.g.*, 0.125), we find I_T such that $f(I_T) = r$. Since the integral has no closed form, we approximate it numerically using a Riemann sum and solve:

$$I_T = \arg \min_{I_T} (f(I_T) - r)^2. \quad (12)$$

Applying Eq. 12, selection ratios r of 0.0625, 0.125, and 0.25 yield corresponding I_T values of 2.06,

Method	Selection Ratio (%)	
	25.0	
	$A_{avg} \uparrow$	$A_{last} \uparrow$
Full-Data Training	72.31±0.42	78.18±0.75
Random	67.44±0.12	74.12±0.42
GradNorm (ICML 2018)	67.91±0.55	73.39±0.30
Self-Sup (NeurIPS 2022)	64.34±0.49	70.71±0.56
COINCIDE (EMNLP 2024)	65.12±0.38	71.04±0.72
DBP (ICLR 2024)	62.42±0.42	72.24±0.61
InfoBatch (ICLR 2024)	65.69±0.30	73.51±0.45
DivBS (ICLR 2024)	66.18±0.74	<u>75.57±0.42</u>
TIVE (arXiv:2403)	64.64±0.59	72.16±0.81
Adapt-∞ (ICLR 2025)	65.95±0.61	72.18±0.16
OASIS (Ours)	70.23±0.27	76.41±0.41

Table 11: **Quantitative comparison on MICVIT benchmark under selection ratio 25.0%.** We use Qwen-VL-2.5-7B as the MLLM. Bold indicates the highest performance; underlined results are within the 0.05 t-test significance level. 'Full-Data Training' uses all data without selection.

1.53, and 0.89, respectively. However, data distribution variations and the probabilistic selection process may cause the actual proportion of selected samples to deviate from the target ratio. To ensure fair comparison with baseline methods, we fine-tune I_T to achieve sample counts that closely approximate but remain marginally below the target selection ratio.

A.7 Different Information Metrics

We compare OASIS using Fisher Information to other metrics for measuring the informativeness I of samples, including Entropy (Coleman et al., 2020), Perplexity (Li et al., 2023b), and EL2N (Paul et al., 2021). As shown in Tab. 12, using sample-wise FI as our Informativeness outperforms other metrics.

Method	MICVIT		COAST	
	$A_{last} \uparrow$	$A_{avg} \uparrow$	$A_{last} \uparrow$	$A_{avg} \uparrow$
Entropy	<u>62.75±0.84</u>	<u>70.08±0.99</u>	22.53±0.46	30.42±0.57
Perplexity	59.86±1.37	64.49±0.72	20.01±0.73	28.64±0.82
EL2N	60.36±1.44	67.15±0.81	23.28±0.56	31.81±0.60
Fisher Information (Ours)	64.39±0.58	71.26±0.72	25.67±0.35	34.23±0.38

Table 12: **Comparison of different information metrics.** On MICVIT and COAST benchmarks, we apply different existing information metrics in place of Fisher Information to OASIS, when selection ratio is 6.25%. Bold indicates the highest performance, and underlined results are within the 0.05 significance level of the t-test.

A.8 Ablation Study on Task Order

In Tab. 13 and Tab. 14, we conduct ablations on three different task orders on COAST and MICVIT, respectively. For each setting, 6.25% of the training data is selected using OASIS or the top three baseline methods. The results demonstrate that regardless of the change in task order, OASIS outperforms other selection methods.

Order	Method	$A_{avg} \uparrow$	$A_{last} \uparrow$
cdim	Random	23.57±0.17	30.80±0.30
	InfoBatch	22.93±0.73	29.14±0.56
	DivBS	23.41±0.14	31.72±0.18
	OASIS (Ours)	25.67±0.35	34.23±0.38
imcd	Random	21.45±0.39	29.25±0.45
	InfoBatch	22.39±0.53	30.04±0.72
	DIVBS	23.84±0.26	31.10±0.56
	OASIS (Ours)	25.01±0.41	33.96±0.53
dmci	Random	22.17±0.42	30.64±0.33
	InfoBatch	20.31±0.25	29.53±1.28
	DIVBS	22.92±0.33	<u>32.31±0.74</u>
	OASIS (Ours)	24.36±0.59	33.28±0.26

Table 13: **Ablation on task order on COAST benchmark.** cdim, imcd, and dmci denote task orders of ChartQA → DocVQA → IconQA → MedicalQA, IconQA → MedicalQA → ChartQA → DocVQA, and DocVQA → MedicalQA → ChartQA → IconQA, respectively.

Order	Method	$A_{avg} \uparrow$	$A_{last} \uparrow$
ONCHoPDH	Random	61.15±0.34	67.29±0.61
	InfoBatch	60.82±0.75	68.88±1.09
	DivBS	61.07±0.58	69.06±0.54
	OASIS (Ours)	64.39±0.58	71.76±0.72
HDPHoCNO	Random	57.85±0.63	66.94±0.74
	InfoBatch	58.04±0.47	67.69±0.80
	DIVBS	58.39±0.28	69.32±0.53
	OASIS (Ours)	61.87±0.82	70.98±0.64
PNHOHoCD	Random	60.31±0.88	68.18±0.62
	InfoBatch	60.25±0.35	67.52±0.16
	DIVBS	61.70±0.74	69.16±0.43
	OASIS (Ours)	63.12±0.58	71.31±0.91

Table 14: **Ablation on task order on MICVIT benchmark.** ONCHoPDH, HDPHoCNO, and PNHOHoCD denote task orders of Bongard-OpenWorld → NLVR2 → Co-Instruct-DB, Bongard-HOI → PatternCom → DVQA → HQ Edit, HQ Edit → DVQA → PatternCom → Bongard-HOI → NLVR2 → Bongard-OpenWorld, and PatternCom → NLVR2 → HQ Edit → Bongard-Openworld → Bongard-HOI → Co-Instruct-DB → DVQA, respectively.

A.9 Effect of EMA Ratio α

We further evaluate the effect of EMA ratio α on OASIS, and summarize the results in Tab. 15. As shown, extremely large or small values of α degrade performance: high α fails to capture the informativeness of past batches, while low α overemphasizes outdated informativeness. To balance this trade-off, we use a moderate value of $\alpha = 0.9$ across all benchmarks and selection ratios.

EMA Ratio α	$A_{avg} \uparrow$	$A_{last} \uparrow$
0.7	22.24 \pm 0.25	31.93 \pm 0.75
0.9	24.36 \pm 0.59	33.28 \pm 0.26
0.99	22.80 \pm 0.42	32.73 \pm 0.64
0.999	23.05 \pm 0.57	32.94 \pm 0.81

Table 15: Ablation on EMA ratio.

A.10 Accuracy Over Time

We compare the average accuracy of seen tasks at each time point between our method and baselines. Specifically, we evaluate performance across different selection ratios and benchmarks, with results shown in Fig. 6 and Fig. 7, respectively. As shown in the figures, our method outperforms baselines at all time points, demonstrating that its superior performance is not limited to specific intervals but is consistently maintained throughout the entire CVIT process.

A.11 Comparison of Computational Costs

We compare the computational cost of OASIS with other selection baselines in Tab. 16. As shown, all methods require forward passes over candidate samples. Sample selection methods (*e.g.*, Self-Sup and COINCIDE) that rely solely on features do not incur additional backward pass costs. In contrast, gradient-based methods (*e.g.*, OASIS and GradNorm) involve backward passes to compute sample-wise gradients. However, unlike TIVE and Adapt- ∞ , which introduce substantial overhead due to full-layer gradient computations or intermediate layer calculations, OASIS leverages only the last-layer gradients, resulting in negligible overhead compared to the forward pass (*i.e.*, less than 3.5%).

A.12 Impact Statements

In this work, we focus on advancing online sample selection algorithm for continual visual instruction tuning. Our approach prioritizes training efficiency

while maintaining strong performance, allowing large pre-trained MLLMs to adapt more effectively and make fairer, less biased decisions when processing continuous streams of real-world data.

A.13 Detailed Algorithm of OASIS

We provide a comprehensive pseudocode of OASIS in Algorithm 1.

A.14 Comparison of the Number of Selected Samples

While baselines select a fixed number of samples per batch, thus selecting the same number of total samples, OASIS dynamically selects samples probabilistically. For fair comparison, we ensure our approach uses comparable or fewer total samples than those selected by other baselines. We summarize the selected samples for each baseline in Tab. 17. Despite using fewer samples, our method outperforms the baselines, as demonstrated in Sec. 4.2.

A.15 Data Privacy and Content Sensitivity

For CVIT benchmarks, we use existing datasets such as COAST and Adapt, which have already filtered out privacy-sensitive content, as well as MICVIT, a combination of existing multimodal benchmarks that are also free from sensitive content.

A.16 Potential Risks

In the CVIT setup, real-time data arrives continuously in a streaming manner, leading to imbalanced data distributions at each time step. This can unintentionally introduce bias throughout the training process.

A.17 Parameters for Packages

For evaluation, we measure accuracy, which selects an answer among multiple candidate choices. In ORIS, we normalize the informativeness score I using Z-score normalization based on our empirical evidence from the QQ-plot.

A.18 License For Artifacts

We utilize publicly available data, models, and codebases, as provided by the original papers for each baseline method.

A.19 Use of AI Assistance

We use AI assistance, such as GPT-4, solely for grammatical error corrections.

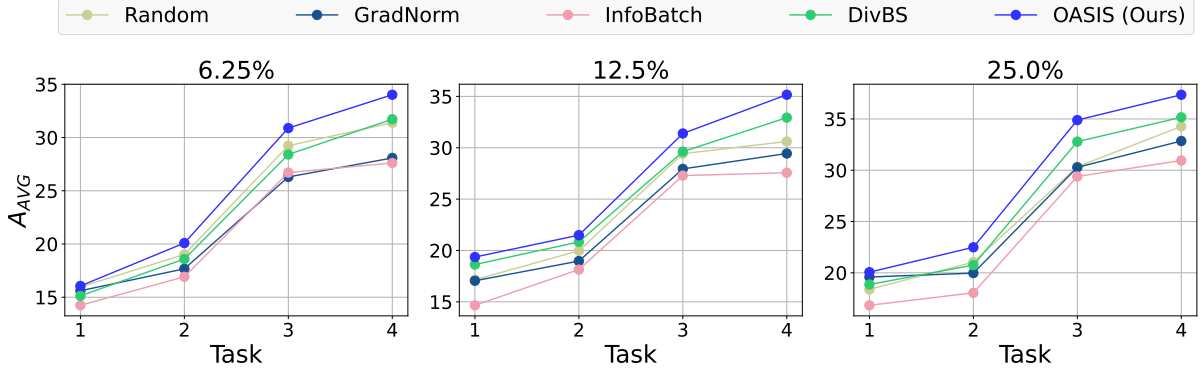


Figure 6: **Average accuracies over time on COAST benchmark under different selection ratios.** Performance at task t denotes the average accuracy over all seen tasks up to that point (*i.e.*, task 1 through task t).

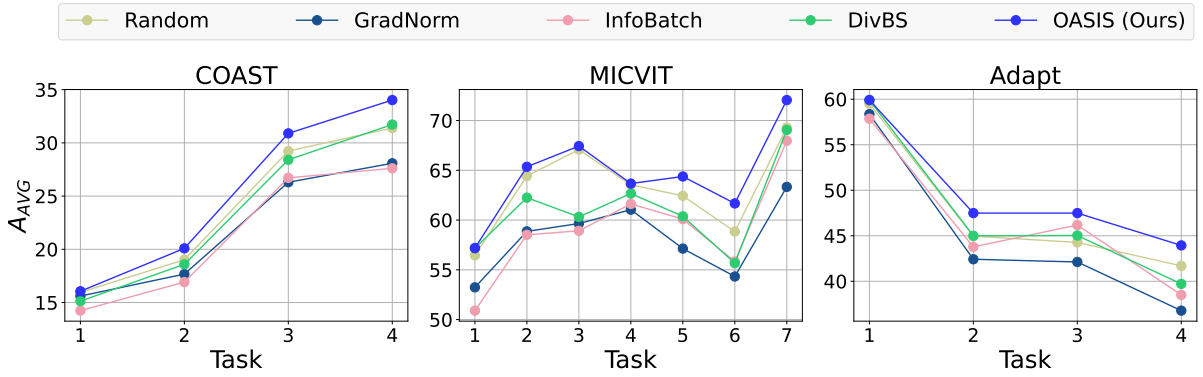


Figure 7: **Average accuracy over time across benchmarks.** Performance at task t denotes the average accuracy over all seen tasks up to that point (*i.e.*, task 1 through task t). We use a selection ratio of 6.25% across all benchmarks.

Methods	Overhead Type	Relative \mathcal{C} to OASIS
GradNorm (ICML 2018)	Forward Pass + Last Layer Gradient Compute	1.000
Self-Sup (NeurIPS 2022)	Forward Pass	0.976
COINCIDE (EMNLP 2024)	Forward Pass	0.976
DBP (ICLR 2024)	Forward Pass	0.976
InfoBatch (ICLR 2024)	Forward Pass	0.976
DivBS (ICML 2024)	Forward Pass + Last Layer Gradient Compute	1.000
TIVE (arXiv:2403)	Forward Pass + Full Layer Gradient Compute	2.038
Adapt- ∞ (ICLR 2025)	Forward Pass + Middle Layer Gradient Compute	1.507
OASIS (Ours)	Forward Pass + Last Layer Gradient Compute	1.000

Table 16: **Comparison of computational costs.** OASIS incurs additional computational cost compared to forward-only baselines (*e.g.*, Self-Sup), but only by approximately 3.4%.

Method	MICVIT			COAST			Adapt		
	6.25%	12.5%	25.0%	6.25%	12.5%	25.0%	6.25%	12.5%	25.0%
Baselines	43394	86788	173576	10000	20000	30000	40000	80000	120000
OASIS (Ours)	43158	86251	173242	9874	19772	29629	39589	79604	119154

Table 17: **Comparison of the number of selected samples.** We compare the average number of selected samples by OASIS across three different seeds with those selected by other sample selection baselines.

Algorithm 1 OASIS

```
1: Input: model  $f_\theta$ , batch  $B_t$ , batch size  $N_B$ , EMA  $\mu_t$ , EMV  $\sigma_t$ , threshold  $I_T$ , number of layers  $L$ 
2: Initialize: Informativeness set  $I^{(t)} \leftarrow \emptyset$ , high informative sample set  $H \leftarrow \emptyset$ 
3: // Stage 1: Calculate Informativeness  $I^{(t)}$  I of each sample in  $B_t$ 
4: for each  $(x_i^{(t)}, y_i^{(t)}) \in B_t$  do
5:   Calculate gradient  $g_i \leftarrow \frac{\partial \ell(d_i^{(t)})}{\partial \theta_L}$ 
6:   Calculate Informativeness  $I_i^{(t)} \leftarrow \text{tr}(g_i \cdot g_i^\top)$ 
7:   Add to set  $I^{(t)} \leftarrow I^{(t)} \cup \{I_i^{(t)}\}$ 
8: end for
9: // Stage 2: SIREN (Similarity-aware Information Redundancy Elimination)
10: Initialize adjusted Informativeness  $\tilde{I}^{(t)} \leftarrow I^{(t)}$ 
11: while  $|H| < N_B$  do
12:   Add most informative sample  $H \leftarrow H \cup \left\{ \arg \max_{d_i^{(t)} \in B_t \setminus H} \tilde{I}_i^{(t)} \right\}$ 
13:   for each  $d_i^{(t)} \in B_t \setminus H$  do
14:     for each  $d_h^{(t)} \in H$  do
15:       Calculate updated Informativeness  $\tilde{I}_i^{(t)} \leftarrow I_i^{(t)} - \cos(g_i, g_h) \cdot I_h^{(t)}$ 
16:     end for
17:     if  $|H| > 1$  then
18:       Account higher-order redundancy due to overlapping similarities between  $d_h^{(t)} \in H$ 
19:        $\tilde{I}_i^{(t)} = \tilde{I}_i^{(t)} + \sum_{\substack{U \subseteq H \\ |U| \geq 2}} (-1)^{|U|} \cos(g_i, \bar{g}_U) \cdot \bar{I}_U^{(t)}$ 
20:     end if
21:   end for
22: end while
23: // Stage 3: Calculate Relative Informativeness  $\hat{I}^{(t)}$ 
24: for each  $\tilde{I}_i^{(t)}$  in  $\tilde{I}^{(t)}$  do
25:   Calculate Relative Informativeness  $\hat{I}_i^{(t)} \leftarrow \frac{\tilde{I}_i^{(t)} - \mu_t}{\sigma_t}$ 
26: end for
27: // Stage 4: Probabilistic Sampling
28: Sample random threshold from uniform distribution  $r \sim \mathcal{U}(0, 1)$ 
29: Select samples  $B^* \leftarrow \{(x_i^{(t)}, y_i^{(t)}) \in B_t \mid \sigma(\hat{I}_i^{(t)} - I_T) > r\}$ 
30: Calculate average Informativeness  $\bar{I}^{(t)} = \frac{1}{N_B} \sum_{i=1}^{N_B} I_i^{(t)}$ 
31: Update EMA  $\mu_t = \alpha \bar{I}^{(t)} + (1 - \alpha) \mu_{t-1}$ 
32: Update EMV  $\sigma_t = \alpha (\bar{I}^{(t)} - \mu_{t-1})^2 + (1 - \alpha) \sigma_{t-1}$ 
33: Output: selected samples  $B^*$ 
```
